

FORMING THE FIRST STARS IN THE UNIVERSE: THE FRAGMENTATION OF  
PRIMORDIAL GASVOLKER BROMM, PAOLO S. COPPI, AND RICHARD B. LARSON  
Department of Astronomy, Yale University, New Haven, CT 06520-8101;  
volker@astro.yale.edu, coppi@astro.yale.edu, larson@astro.yale.edu

## ABSTRACT

In order to constrain the initial mass function (IMF) of the first generation of stars (Population III), we investigate the fragmentation properties of metal-free gas in the context of a hierarchical model of structure formation. We investigate the evolution of an isolated  $3\sigma$  peak of mass  $2 \times 10^6 M_\odot$  which collapses at  $z_{coll} \simeq 30$  using Smoothed Particle Hydrodynamics. We find that the gas dissipatively settles into a rotationally supported disk which has a very filamentary morphology. The gas in these filaments is Jeans unstable with  $M_J \sim 10^3 M_\odot$ . Fragmentation leads to the formation of high density ( $n > 10^8 \text{ cm}^{-3}$ ) clumps which subsequently grow in mass by accreting surrounding gas and by merging with other clumps up to masses of  $\sim 10^4 M_\odot$ . This suggests that the very first stars were rather massive. We explore the complex dynamics of the merging and tidal disruption of these clumps by following their evolution over a few dynamical times.

*Subject headings:* cosmology: theory — early universe — galaxies: formation — hydrodynamics

## 1. INTRODUCTION

Little is known about the history of the universe at redshifts  $z \simeq 1000 - 5$ , corresponding to  $10^6 - 10^9$  years after the Big Bang, and only recently have astrophysicists begun to seriously investigate this crucial post-recombination era. At  $z \sim 1000$ , the photons of the cosmic microwave background (CMB) shifted into the infrared, and the universe entered what has been termed the “Dark Ages” (Rees 1999). We know that the universe was reionized again before a redshift of  $\sim 5$  from the absence of Gunn-Peterson absorption in the spectra of high redshift quasars. One of the grand challenges in modern cosmology is to determine when the universe was lit up again by the first luminous objects (the so-called Population III) which were responsible for reionizing and reheating the intergalactic medium (Haiman & Loeb 1997; Ferrara 1998). The very first generation of stars must have formed out of probably unmagnetized, pure H/He gas, since heavy elements can only be produced in the interior of stars. These characteristics render the primordial star formation problem very different from the present-day case, and lead to a significant simplification of the relevant physics (Larson 1998; Loeb 1998).

To determine the characteristic mass scale of the Population III stars, and to constrain their initial mass function (IMF), one has to study the collapse and fragmentation of metal-free gas. This problem has been addressed by a number of authors (e.g., Yoneyama 1972; Hutchins 1976; Carlberg 1981; Kashlinsky & Rees 1983; Palla, Salpeter, & Stahler 1983; Silk 1983; Haiman, Thoul, & Loeb 1996; Uehara et al. 1996; Tegmark et al. 1997; Omukai & Nishi 1998; Nakamura & Umemura 1999). Recently, three-dimensional cosmological simulations have reached sufficient resolution on very small scales to approach the Population III star formation problem (Anninos & Norman 1996; Ostriker & Gnedin 1996; Abel et al. 1998a).

Complementary to these last studies, we explore the fragmentation of primordial gas under a variety of initial

conditions. Our method allows us to follow the evolution of the fragments for a few dynamical times, and to include the physics of competitive accretion. These capabilities are crucial for the investigation of the resulting mass spectrum. A more detailed exposition of our code, together with further results of our exploratory survey, will be presented in a forthcoming publication (Bromm, Coppi, & Larson 1999). In this Letter, we focus on one representative experiment which addresses the key question: *How does the fragmentation of the first collapsing gas clouds proceed in a hierarchical (bottom up) scenario of structure formation?*

## 2. NUMERICAL METHOD

Our code is based on a version of TREESPH (Hernquist & Katz 1989) which combines the Smoothed Particle Hydrodynamics (SPH) method (e.g., Monaghan 1992) with a hierarchical (tree) gravity solver. To study primordial gas, we have made a number of additions. Most importantly, radiative cooling due to hydrogen molecules has been taken into account. In the absence of metals,  $\text{H}_2$  is the main coolant below  $\sim 10^4$  K, the typical temperature range in collapsing Population III objects. We implement the  $\text{H}_2$  cooling function given by Galli & Palla (1998). At temperatures approaching  $10^4$  K, cooling due to lines of atomic hydrogen dominates (Katz & Gunn 1991). The efficiency of  $\text{H}_2$  cooling is very sensitive to the  $\text{H}_2$  abundance. Therefore, it is necessary to compute the nonequilibrium evolution of the primordial chemistry. We take into account the six species H,  $\text{H}^+$ ,  $\text{H}^-$ ,  $\text{H}_2$ ,  $\text{H}_2^+$ , and  $\text{e}^-$ . Helium is neglected, since the temperatures in our application are low enough ( $< 10^4$  K) to render the He species almost inert. Reaction rates are taken from Haiman et al. (1996). In addition, we have included 3-body reactions which become important at high density ( $n > 10^8 \text{ cm}^{-3}$ ), and can convert the gas almost completely into molecular form (Palla et al. 1983). The chemistry network is solved by the approximate backwards differencing formula (BDF) method (Anninos et al. 1997).

We have devised an algorithm to merge SPH particles in high density regions to overcome the otherwise prohibitive timestep limitation, as enforced by the Courant stability criterion (Bate, Bonnell, & Price 1995). To follow the simulation for a few dynamical times, we allow SPH particles to merge into more massive ones, provided they exceed a pre-determined density threshold, typically  $10^8 - 10^{10} \text{ cm}^{-3}$ . More details of the merging algorithm will be given in Bromm et al. (1999).

### 3. THE SIMULATION

#### 3.1. Initial Conditions

Within a hierarchical cosmogony, the very first stars are expected to form out of  $3 - 4\sigma$  peaks in the random field of primordial density fluctuations. The early (linear) evolution of such a peak, assumed to be an isolated and roughly spherical overdensity, can be described by the top-hat model (e.g., Padmanabhan 1993). We use the top-hat approximation to specify the initial dark matter (DM) configuration, where we choose the background universe to be described by the critical Einstein-de Sitter solution with density parameters:  $\Omega_{DM} = 0.95$ ,  $\Omega_B = 0.05$ , and Hubble constant  $h = H_0/(100 \text{ km s}^{-1} \text{ Mpc}^{-1})=0.5$ . In this paper, we investigate the fate of a  $3\sigma$  peak of total mass  $2 \times 10^6 M_\odot$ , corresponding to  $10^5 M_\odot$  in baryons which is close to the cosmological Jeans mass (Couchman & Rees 1986). On this mass scale, the standard Cold Dark Matter (CDM) scenario predicts a present-day r.m.s. overdensity of  $\sigma_0(M) \simeq 16$ , with a normalization  $\sigma_8 = 1$  on the  $8h^{-1} \text{ Mpc}$  scale. Then, one can estimate the redshift of collapse (or virialization) from:  $1+z_{coll} = 3\sigma_0(M)/1.69$ , leading to  $z_{coll} \simeq 30$ . Our simulation is initialized at  $z_i = 100$ , by performing the following steps.

The collisionless DM particles are placed on a cubical Cartesian grid, and are then perturbed according to a given power spectrum  $P(k) = Ak^n$ , by applying the Zel'dovich approximation (Zel'dovich 1970) which also allows to self-consistently assign initial velocities. The power-law index is set to  $n = -3$  which is the asymptotic small-scale behavior in the standard CDM model (Peebles 1993). The amplitude  $A$  is adjusted, so that the fundamental mode (i.e., the smallest contributing wavenumber  $k_{min}$ ), has an initial mean square overdensity which grows to  $P(k_{min}) \simeq 1$  at collapse. Next, particles within a (proper) radius of  $R_i = 150 \text{ pc}$  are selected for the simulation. The resulting number of DM particles is  $N_{DM} = 14123$ . Finally, the particles are set into rigid rotation and are endowed with a uniform Hubble expansion (see also Katz 1991). Angular momentum is added by assuming a spin-parameter  $\lambda = L|E|^{1/2}/(GM^{5/2}) = 0.05$ , where  $L$ ,  $E$ , and  $M$  are the total angular momentum, energy, and mass, respectively.

The collisional SPH particles ( $N_{SPH} = 16384$  in this simulation) are randomly placed to approximate a uniform initial density. The random sampling inevitably introduces shot-noise. The DM particles were set up on a regular grid specifically to avoid the unphysical shot-noise distribution which could mask the desired physical power spectrum. For the gas, however, the presence of the shot noise is not a big problem, since the gas mass is initially smaller than the Jeans mass. Therefore, sound waves will efficiently wipe out all initial density disturbances. The

SPH particles are endowed with the same Hubble expansion and rigid rotation as the DM ones. Since  $z < 100$ , heating, cooling, and photoreactions due to the CMB can be safely neglected here. For the chemical abundances and the gas temperature, we adopt the initial values (see Tegmark et al. 1997):  $x_i = 4.6 \times 10^{-4}$ ,  $f_i = 10^{-4}$ , and  $T_{gas,i} \simeq 200 \text{ K}$ , where  $x_i$ ,  $f_i$  are the initial free electron and  $\text{H}_2$  abundances, respectively. The use of a more realistic rate for the photodissociation of  $\text{H}_2^+$  predicts a lower initial  $\text{H}_2$  abundance, typically  $f_i \simeq 10^{-6}$ . The evolution of a simulation initialized with such a lower value, however, quickly converges to the case presented in this paper.

#### 3.2. Results

##### 3.2.1. Free-fall Phase

From turnaround ( $z = 50$ ) to the moment of collapse ( $z \simeq 30$ ), both the DM and the gas are freely falling. In response to the initially imprinted  $P(k) \propto k^{-3}$  noise, the DM develops marked substructure. This happens in a hierarchical fashion, where smaller clumps form first, and rapidly merge into larger aggregations. The gas initially falls together with the DM, heating up adiabatically,  $T \propto n^{2/3}$  for  $\gamma = 5/3$ , until the temperature reaches the virial value of  $T_{vir} \sim 5000 \text{ K}$  which is determined by the depth of the DM potential well. The virialized gas is able to cool efficiently, and the temperature decreases again with continuing compression down to a few  $100 \text{ K}$ . At first, the gas is not able to condense onto the shallow DM potential wells, and its mass distribution remains smooth. In the course of the collapse, however, the baryonic Jeans mass decreases enough to eventually allow the gas to fall into the deepening DM troughs. This gravitational ‘‘head-start’’ is important because it determines where fragmentation occurs first, resulting in the most massive gas clumps.

Briefly after collapse, all the substructure in the DM has been wiped out in the process of violent relaxation (Lynden-Bell 1967) which is very effective in quickly establishing virial equilibrium on the dynamical timescale of the DM halo ( $\sim 10^7$  years). Before having been wiped out, however, the DM substructure has left its imprint on the gas, determining the morphology of the incipient disk. The DM reaches an equilibrium configuration with a core radius of  $\sim 10 \text{ pc}$  and an approximately isothermal density profile ( $\rho \propto r^{-2}$ ) further out.

The central gas disk is horizontally supported by rotation. In the presence of a DM halo, one expects a contraction by a factor of  $1/\lambda \simeq 20$  for rotational support. The dimension of the disk, as shown in Figure 2, is in good accordance with this prediction. Vertically, the disk is roughly pressure supported with a scale height of  $H = c_s^2/(G\Sigma) \simeq 2 \text{ pc}$ , where  $c_s \simeq 2 \text{ km/s}$  is the sound speed, and  $\Sigma$  the gas surface density. The resulting disk has a very filamentary and knotty structure with typical densities of  $n \sim 10^4 \text{ cm}^{-3}$  and temperatures of  $T \sim 500 \text{ K}$ , corresponding to a Jeans mass of  $M_J \sim 10^3 M_\odot$ . We next discuss the fragmentation of these filamentary features.

##### 3.2.2. Disk-like Phase

The gas which makes up the filaments is Jeans unstable since  $t_{ff} < t_{sound}$ , where the free-fall time is  $t_{ff} \simeq (Gm_{HN})^{-1/2}$ , and the sound-crossing time  $t_{sound} \simeq R/c_s$ .  $R \sim 15 \text{ pc}$  is the radius of the disk. In Figure 1, the free-

fall time is compared to the sound-crossing time and to the cooling time,  $t_{cool} \simeq nk_B T / (fn^2 L)$ . Here,  $f$  is the fractional  $H_2$  abundance, and  $L$  the cooling rate (in  $\text{erg s}^{-1} \text{cm}^3$ ). For densities  $n > 10^3 \text{ cm}^{-3}$ , the gas becomes Jeans unstable. The onset of instability roughly coincides with the condition that  $t_{cool} \simeq t_{ff}$ . The value  $n \sim 10^3 \text{ cm}^{-3}$  is also the critical density for the rotational-vibrational levels of  $H_2$  being populated according to local thermodynamic equilibrium (LTE).

The first regions to undergo runaway collapse lead to the formation of dense ( $n > 10^8 \text{ cm}^{-3}$ ) gas clumps of mass  $\sim 10^3 M_\odot$ . The dynamical state of a typical clump can be described by the ratios  $E_{th}/|E_{grav}| \simeq 0.5$ , and  $E_{rot}/|E_{grav}| \simeq 0.1$ , where  $E_{th}$ ,  $E_{rot}$ ,  $E_{grav}$  are the thermal, rotational, and gravitational energies of the clump. The further evolution of the disk consists of a complex history of new clumps forming, and old ones continually accreting gas and occasionally merging with other clumps. The outcome of this evolution is shown in Figure 2, corresponding to the situation at  $z = 28$ . The disk-like structure has fragmented into 13 clumps, ranging in mass from 220 to  $\sim 10^4 M_\odot$ . At this stage,  $\sim 50\%$  of the total gas mass has been incorporated into high density clumps. This fraction is unrealistically high due to the homologous nature of the top-hat collapse where all particles reach the center at the same time. Abel et al. (1998a), on the other hand, estimate this fraction to be  $\sim 8\%$ . This value is more realistic, since these authors consider an overdensity which is initially already centrally concentrated, leading to a collapse which is spread out in time. Since the larger clumps tend to retain their individuality, the final evolutionary state of the disk is expected to be a small cluster of isolated clumps.

Figure 3 summarizes the thermodynamic state of the gas together with the chemical abundances. When a region undergoes runaway collapse, particles are drawn from the quasi-stationary ‘‘reservoir’’ at  $n \sim 10^4 \text{ cm}^{-3}$  which corresponds to the filamentary gas, and swiftly move to higher densities at roughly constant temperature (Fig. 3c). At a density of  $n = 10^8 \text{ cm}^{-3}$ , SPH particles are merged into more massive ones, as described in §2. At higher densities, the Jeans mass would decrease below the resolution limit ( $M_{res} \sim 200 M_\odot$ ; Bate & Burkert 1997) of our simulation (Fig. 3d). In order to reliably follow the evolution of the gas to even higher densities, a larger number of SPH particles would be needed. In this case, one would expect the gas density to increase up to the point where the now fully molecular gas becomes opaque, and subsequently behaves adiabatically again. The present study, however, has the purpose of following the evolution of many gas clumps for a few dynamical times. Therefore, merging at some point

is inevitable.

#### 4. SUMMARY AND CONCLUSIONS

We have discussed the evolution of a primordial star forming region in the context of the standard CDM model for structure formation. In the early stages of the collapse, the morphology of the DM substructure imprints a pattern onto the initially completely smooth gas which determines where gas fragmentation is to occur first. Therefore, the initial power spectrum of the DM fluctuations might be an important ingredient for primordial star formation. Simultaneously with the virialization of the DM component, the gas dissipatively settles down into a compact central disk. This disk has a very filamentary structure, and is Jeans unstable which leads to fragmentation into clumps of initially  $\sim 10^2 - 10^3 M_\odot$ . These clumps grow in mass by both accreting surrounding gas, and by merging with other high-density clumps. At the end of this process, a small number ( $\sim 10$ ) of these clumps have formed.

Population III stars, then, might have been quite massive, perhaps even ‘‘very massive’’ ( $M_{char} > 100 M_\odot$ ), if one assumes that a Jeans mass clump does not undergo significant further fragmentation. Although subsequent fragmentation cannot be excluded, this is expected to lead to the formation of a binary or a small multiple system, if experience from present-day star formation offers any guidance here (Larson 1998). Our results agree well with those of Abel, Bryan, & Norman (1998b) who have applied the Adaptive Mesh Refinement (AMR) method to the problem. These authors find a dense core of order a few times  $10^2 M_\odot$ , which continues to accrete mass and shows no sign of further subfragmentation. Clearly, high resolution studies of the further clump evolution are necessary, including a treatment of opacity effects (see Omukai & Nishi 1998). We are presently engaged in doing so and will present our findings in a future publication.

The effects of cooling due to HD molecules (Galli & Palla 1998), and of the presence of the CMB on the  $H_2$  level populations (Capuzzo-Dolcetta, Di Fazio, & Palla 1991), were not included in our work, and both could affect the estimate of the Jeans mass. Test calculations indicate that the effect of HD cooling may not significantly change our results, but a more complete treatment will be incorporated in subsequent work.

We would like to thank Z. Haiman and A. Loeb for providing us with their chemical reaction rates and for helpful discussions, L. Hernquist for making available to us a version of TREESPH, and T. Abel, A. Ferrara, and F. Palla for detailed comments. Support from the NASA ATP grant NAG5-7074 is gratefully acknowledged.

#### REFERENCES

- Abel, T., Anninos, P., Norman, M. L., & Zhang, Y. 1998a, *ApJ*, 508, 518  
 Abel, T., Bryan, G. L., & Norman, M. L. 1998b, preprint, (astro-ph/9810215)  
 Anninos, P., & Norman, M. L. 1996, *ApJ*, 460, 556  
 Anninos, P., Zhang, Y., Abel, T., & Norman, M. L. 1997, *NewA*, 2, 209  
 Bate, M. R., Bonnell, I. A., & Price, N. M. 1995, *MNRAS*, 277, 362  
 Bate, M. R., & Burkert, A. 1997, *MNRAS*, 288, 1060  
 Bromm, V., Coppi, P. S., & Larson, R. B. 1999, in preparation  
 Capuzzo-Dolcetta, R., Di Fazio, A., & Palla, F. 1991, *A&AS*, 88, 451  
 Carlberg, R. G. 1981, *MNRAS*, 197, 1021  
 Couchman, H. M. P., & Rees, M. J. 1986, *MNRAS*, 221, 53  
 Ferrara, A. 1998, *ApJ*, 499, L17  
 Galli, D., & Palla, F. 1998, *A&A*, 335, 403  
 Haiman, Z., Thoul, A. A., & Loeb, A. 1996, *ApJ*, 464, 523  
 Haiman, Z., & Loeb, A. 1997, *ApJ*, 483, 21  
 Hernquist, L., & Katz, N. 1989, *ApJS*, 70, 419  
 Hutchins, J. B. 1976, *ApJ*, 205, 103  
 Kashlinsky, A., & Rees, M. J. 1983, *MNRAS*, 205, 955  
 Katz, N. 1991, *ApJ*, 368, 325  
 Katz, N., & Gunn, J. E. 1991, *ApJ*, 377, 365

- Larson, R. B. 1998, MNRAS, 301, 569
- Loeb, A. 1998, in ASP Conf. Ser. 133, Science with the Next Generation Space Telescope, ed. E. Smith & A. Koratkar (San Francisco: ASP), 73
- Lynden-Bell, D. 1967, MNRAS, 136, 101
- Monaghan, J. J. 1992, ARA&A, 30, 543
- Nakamura, F., & Umemura, M. 1999, ApJ, 515, 239
- Omukai, K., & Nishi, R. 1998, ApJ, 508, 141
- Ostriker, J. P., & Gnedin, N. Y. 1996, ApJ, 472, L63
- Padmanabhan, T. 1993, Structure Formation in the Universe (Cambridge: Cambridge Univ. Press), 273
- Palla, F., Salpeter, E. E., & Stahler, S. W. 1983, ApJ, 271, 632
- Peebles, P. J. E. 1993, Principles of Physical Cosmology (Princeton: Princeton Univ. Press), 625
- Rees, M. J. 1999, in AIP Conf. Proc. 470, After the Dark Ages: When Galaxies were Young (the Universe at  $2 < z < 5$ ), ed. S. S. Holt & E. Smith (Woodbury: AIP), 13
- Silk, J. 1983, MNRAS, 205, 705
- Tegmark, M., Silk, J., Rees, M. J., Blanchard, A., Abel, T., & Palla, F. 1997, ApJ, 474, 1
- Uehara, H., Susa, H., Nishi, R., Yamada, M., & Nakamura, T. 1996, ApJ, 473, L95
- Yoneyama, T. 1972, PASJ, 24, 87
- Zel'dovich, Y. B. 1970, A&A, 5, 84

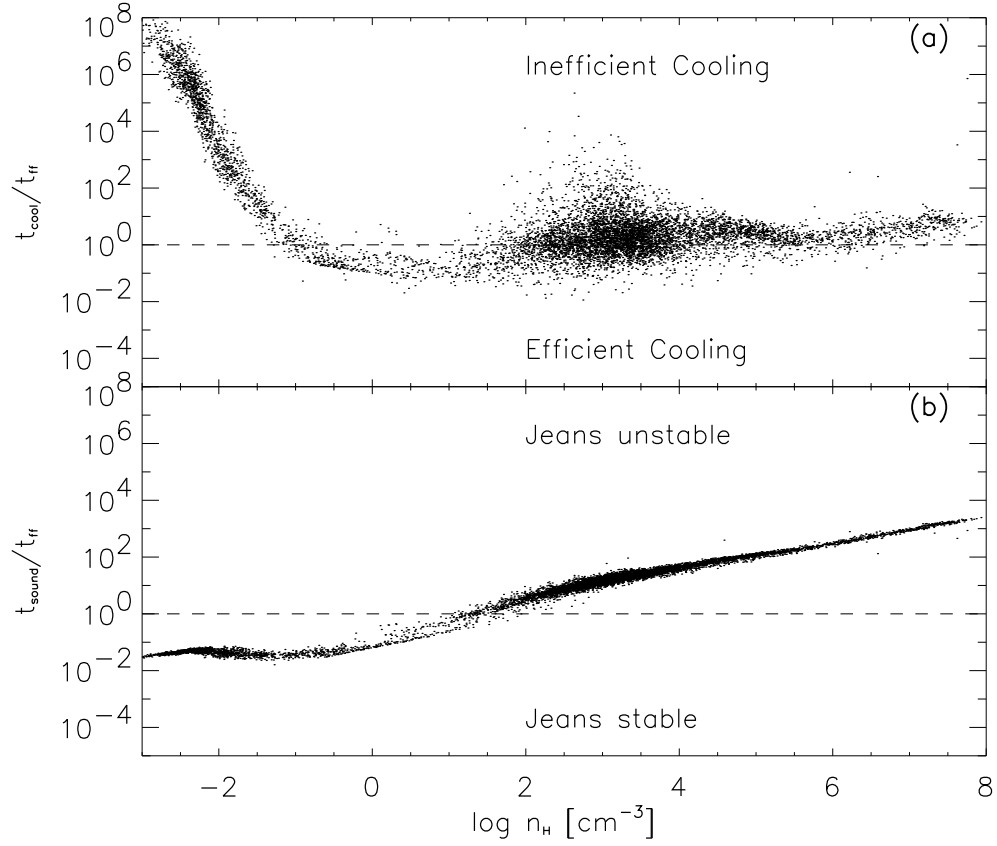


FIG. 1.— Important timescales at  $z = 28$ . **(a)** Ratio of cooling and free-fall timescales vs. gas density. At low density, cooling is not efficient and contraction proceeds adiabatically. For higher densities, characteristic of the gas after virialization, cooling is very efficient up to densities  $n \sim 10^3 \text{ cm}^{-3}$ . The evolution from  $n \sim 10^3 \text{ cm}^{-3}$  to  $n \sim 10^8 \text{ cm}^{-3}$  proceeds such that  $t_{cool} \simeq t_{ff}$ . **(b)** Ratio of sound-crossing and free-fall timescales vs. gas density. For  $t_{ff} < t_{sound}$ , the gas is Jeans unstable. Gravitational instability sets in at  $n \sim 10^3 \text{ cm}^{-3}$  which corresponds to the compressed gas in the disk-like configuration. The onset of instability roughly coincides with the condition that  $t_{cool} \simeq t_{ff}$  in panel (a).

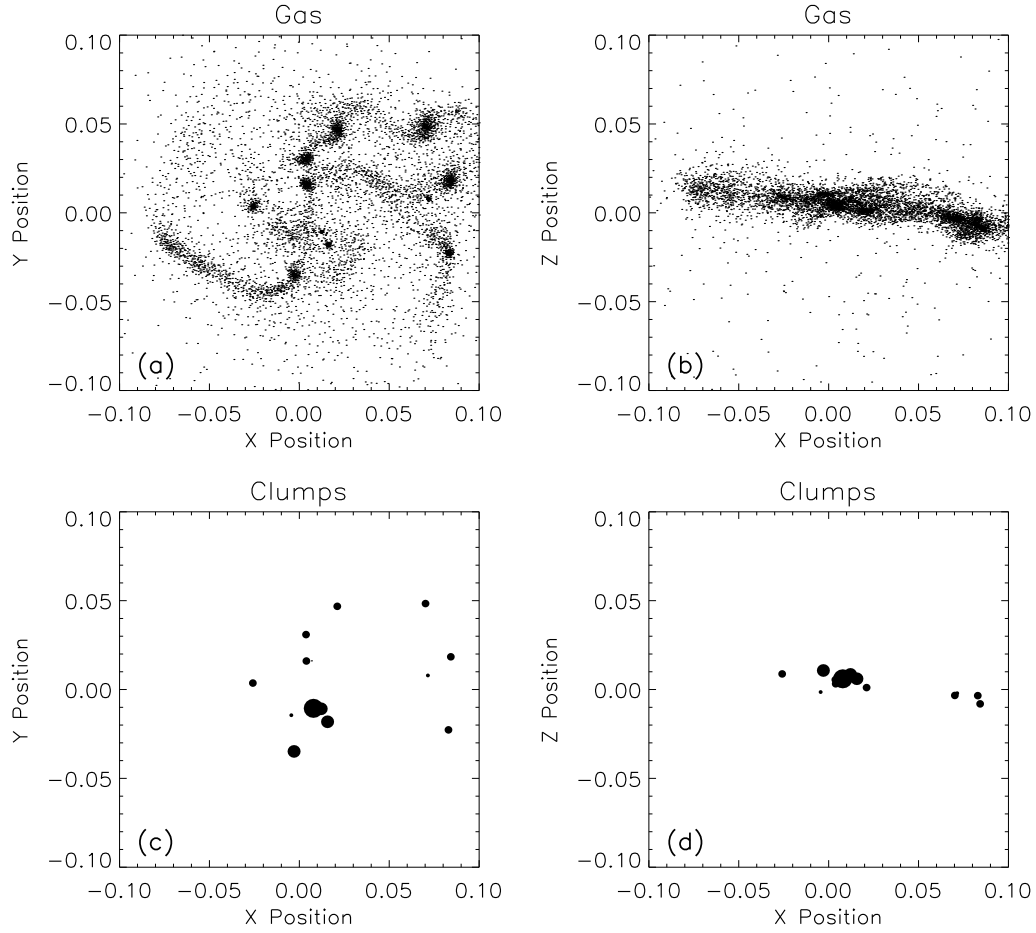


FIG. 2.— Situation at  $z = 28$ . Shown is the ongoing fragmentation of the gas disk in the center of the DM halo. The (proper) length of the box is 30 pc. *Left Panels:* Face-on view. *Right Panels:* Edge-on view. **(a)-(b)** Gas component. The gas which had been assembled in a disk-like configuration, has undergone further fragmentation into roughly spherical high-density ( $n > 10^8 \text{ cm}^{-3}$ ) clumps. **(c)-(d)** Clump distribution. The four increasing dot sizes denote increasing mass scale:  $10^2 - 10^3 M_\odot$ ,  $10^3 - 5 \times 10^3 M_\odot$ ,  $5 \times 10^3 - 10^4 M_\odot$ , and  $M > 10^4 M_\odot$ . By now,  $\sim 50\%$  of the total gas mass is incorporated into high-density clumps. The most massive clumps have already accreted all of the surrounding gas. This explains the paucity of unmerged gas particles close to the center of the disk in panel (a).

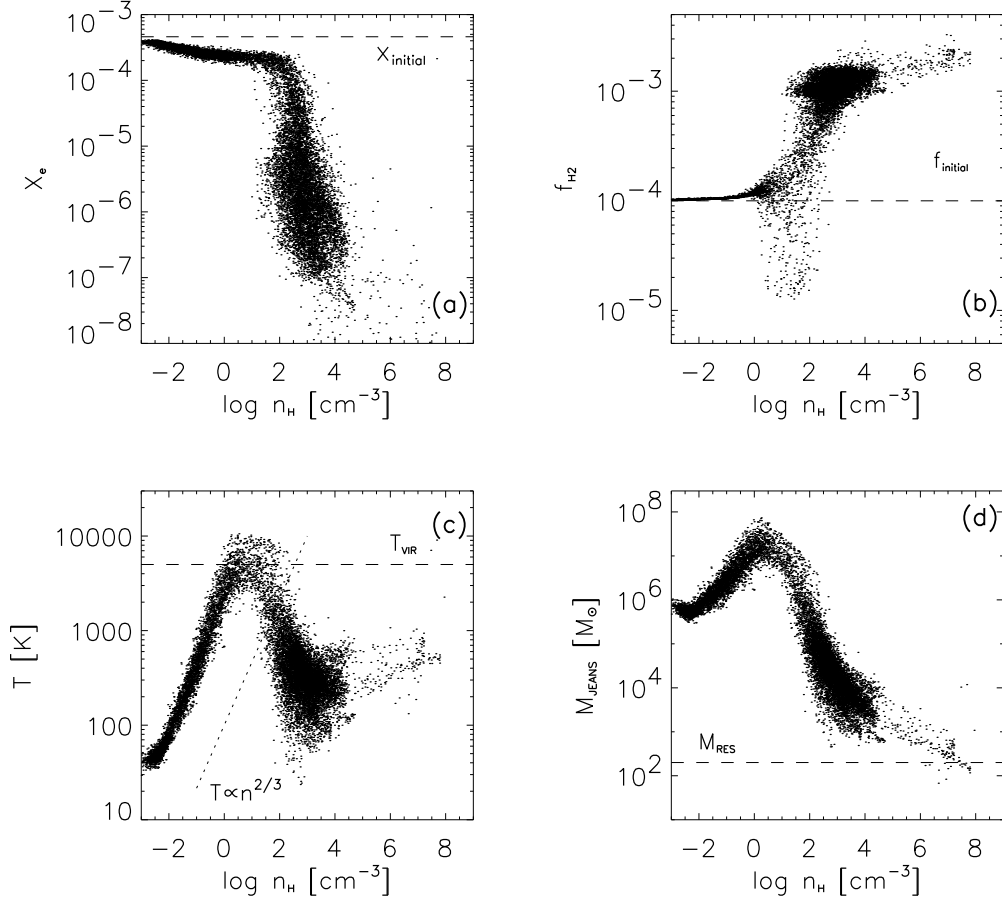


FIG. 3.— Gas properties at  $z = 30.5$ . **(a)** Free electron abundance vs. gas number density. At high density, the residual electrons recombine until the gas is almost completely neutral (at  $n \sim 10^4 \text{ cm}^{-3}$ ). **(b)**  $\text{H}_2$  abundance vs. gas number density. Due to the  $\text{H}^-$  channel, the asymptotic value of  $\sim 10^{-3}$  has been reached for densities  $n > 10^3 \text{ cm}^{-3}$ . **(c)** Gas temperature vs. number density. At low gas densities, the temperature rises due to adiabatic compression until it reaches the virial value. At higher densities,  $\text{H}_2$  line cooling drives the temperature down again until the gas settles into a quasi-equilibrium state at  $T \simeq 500 \text{ K}$  and  $n \simeq 10^4 \text{ cm}^{-3}$ . **(d)** Jeans mass vs. number density. The Jeans mass reaches a value of  $M_J \simeq 10^3 M_{\odot}$  in the disk-like central feature, and approaches the resolution limit of the simulation,  $M_{\text{RES}} \sim 200 M_{\odot}$ , for densities close to the merging threshold of  $n = 10^8 \text{ cm}^{-3}$ .